

Practical Receding-Horizon Optimization Control of the Air Handling Unit in HVAC Systems

Min Xu,[†] Shaoyuan Li,^{*,†} and Wenjian Cai[‡]

Institute of Automation, Shanghai Jiao Tong University, 1954 Hua-Shan Road, Shanghai 200030, People's Republic of China, and School of Electrical and Electronic Engineering, Nanyang Technological University, Singapore 639798, Singapore

This paper is concerned with air handling units (AHUs), the performances of which directly influence those of heating, ventilation and air conditioning systems. An autotuning receding-horizon optimization method is proposed to synthesize a proportional–integral–derivative (PID) type controller for AHUs. This algorithm is composed of two levels of control. The lower level adopts a conventional PID controller to obtain an acceptable, but not necessarily optimal, performance. The higher level provides optimal low-level controller parameters through minimization of the generalized predictive control criterion. Because the method does not require changes in hardware and the definitions of conventional controller parameters, it can be both easily accepted by process engineers and widely applied to industrial areas. Compared with the performance of a well-tuned conventional PID controller, simulation and experimental results show that the proposed method for AHU systems can achieve a better performance under a wide range of operating conditions.

1. Introduction

A typical centralized heating, ventilation and air conditioning (HVAC) system is comprised of five loops: namely, condenser water loop, chilled water loop, chillers, indoor air loop, and air handling unit.¹ Because the performances of air handling units (AHUs) directly influence those of HVAC systems, a good control strategy for AHUs is very critical. Also, because of both the nonideal actuator and system constraints, the HVAC system is highly nonlinear, and so a satisfying controller is difficult to design. Currently, conventional proportional–integral–derivative (PID) controllers are widely used in most AHU processes because of their simplicity and effectiveness.² To improve AHUs' performances for a wide range of operating conditions, tuning methods for PID controller parameters and advanced algorithms have been developed in recent years.

The most common PID advancement in industry is gain scheduling, which can overcome nonlinear process characteristics through tailoring of controller gains over local operating conditions. However, this scheduling is complicated because detailed process knowledge is necessary to define operating conditions and open-loop tests, in which the controller gain within each condition must be locally calibrated.³

Many advanced process control algorithms have been developed for HVAC systems, such as fuzzy control,⁴ neural network,⁵ evolutionary algorithm,⁶ genetic algorithm,⁷ autotuning (AT),⁸ and model predictive control (MPC).⁹ Among those control algorithms, MPC technology has a bright future of industrial application, as shown by a survey that has indicated that MPC technology has more than 2000 applications to date.¹⁰

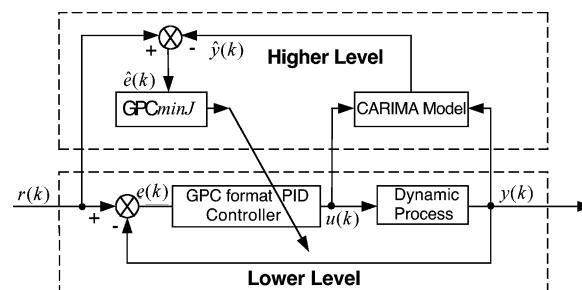


Figure 1. Control structure diagram.

Virk and Loveday¹¹ proposed a predictive on–off control method with both on and off states essentially to determine which gives the smaller prediction error at the next sampling instant. Their experimental data showed that 17% energy can be saved compared with a conventional on–off control algorithm. Jorgl and Pargfrieder¹² presented a fuzzy controller, whose parameters are tuned based on the generalized predictive control (GPC) algorithm, aimed at maximizing user comfort as well as minimizing energy consumption. Cho and Zaheer¹³ developed a predictive control strategy with higher energy efficiency, where the heat supply hours per day are determined based on a forecast of hourly outdoor temperatures. Even though the above methods can improve the HVAC system performance, the controllers are very often too complicated and difficult to facilitate in real-world systems.

In this paper, an AT two-level scheme, which is composed of a receding-horizon optimizer and a time-varying PID controller, is proposed for the AHU system. As shown in Figure 1, there are two levels, a lower level and a higher level. The lower level loop adopts a conventional PID controller, the initial setting of which is specified by process engineers. Also, the higher level loop exploits the receding-horizon optimization strategy to update the lower level controller parameters based on the minimization of the GPC criterion. Assuming that the system is linear and time-invariant or operating

* To whom correspondence should be addressed. Tel.: +86-(21)-6293-2114. Fax: +86-(21)-6293-2145. E-mail: syli@sjtu.edu.cn.

[†] Shanghai Jiao Tong University.

[‡] Nanyang Technological University.

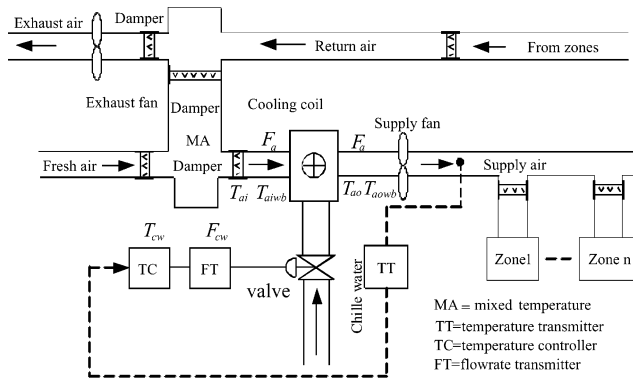


Figure 2. Schematic diagram of an AHU cooling-coil system.

conditions are in a narrow range, this controller structure simplifies a conventional PID controller with well-tuned parameters. Once operating conditions have a large variation, causing the system parameters change, the receding-horizon optimization strategy calculates a new optimal control action and delivers it to the lower level controller. On the basis of cooling-coil models with different load conditions, simulation results exhibit better performances compared with a well-tuned conventional PID controller. Also, experiments on a real-time AHU system demonstrate that a fast setting time and a small overshoot can be obtained by the proposed strategy, even in the presence of disturbance. Because the method does not require changes in hardware and the definitions of conventional controller parameters, it can be both easily accepted by process engineers and widely applied to industrial areas.

2. Control Problem of the AHU

Figure 2 only shows a schematic diagram of a cooling-coil system, which consists of cooling coils, air dampers, fans, chilled water pumps, and valves. Fresh air enters the AHU through the outdoor air damper, depending on the mixing box damper settings. It may be mixed with return air passing through the recirculation air damper. Return air is drawn from each zone by the return fan and is either exhausted or recirculated, depending on the positions of the mixing box dampers. Hence, the conditions at the exit of the mixed air plenum are determined by both the temperatures and flow rates of the outdoor and recirculation air streams. Then, air exiting the mixed air plenum passes through the cooling coils. After being conditioned in the coils, the air is then distributed to each zone through the supply air ductwork.

One of the primary purposes of an AHU is to distribute conditioned air to the occupied zones of a building and maintain T_{ao} at the set-point value. To provide a comfortable environment for occupants, the supply air to a particular zone must offset cool loads imposed on that zone. Therefore, the cool load condition is an important factor affecting system output T_{ao} . Because the cool loads for each zone can vary markedly, system parameters may change with it. However, a conventional PID control scheme is favorable in cases where system parameters are fixed or varying in a narrow range, whereas it is not suitable for AHUs of a large building coping with a wide range of operating conditions and characterized with different model parameters under different cool load conditions.

Furthermore, the cooling-coil system exhibits strong nonlinear characteristics. A dynamic cooling-coil model

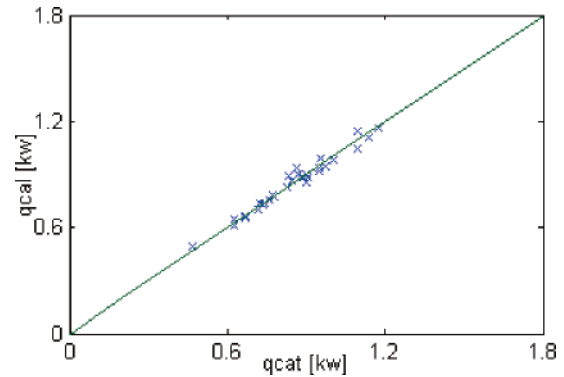


Figure 3. Fitting result of the AHU model.

is proposed in the part that is based on a static-state model developed by Lu and Cai.¹⁴ The static-state model of cooling-coil and energy balance equations can be written as

$$Q = \frac{c_1 F_a^e}{1 + c_2 (F_a / F_{cw})^e} (T_{ai} - T_{cwi}) \quad (1)$$

and

$$Q = c_{cw} F_{cw} (T_{cwo} - T_{cwi}) = c_a F_a (T_{ai} - T_{ao}) \quad (2)$$

where Q is the cooling load, c_{cw} and c_a are the specific heats of chilled water and air, and c_1 , c_2 , and e are AHU system parameters. T_{ai} , T_{aiwb} , and F_a are the dry-bulb temperature, the wet-bulb temperature, and the cooling-coil air flow in the on-coil state, respectively. Likewise, the above variables are noted as T_{ao} and T_{aowb} in the off-coil state. When eqs 1 and 2 are combined, T_{ao} can be described as

$$T_{ao} = T_{ai} - \frac{(c_1/c_a) F_a^{e-1} F_{cw}^e}{F_{cw} + c_2 F_a^e} (T_{ai} - T_{cwi})$$

If $e = 0.6$ (engineering rule of thumb value) is adopted, the model only has two parameters, c_1 and c_2 , to be determined. The fitting result of eq 1 with the parameters $c_1 = 0.45$, $c_2 = 0.7$, and $e = 0.61$ is shown in Figure 3, and the system has nonlinear characteristics with the parameters of T_{ao} , F_{cw} , and F_a . Assuming that the air flow rate F_a acts as a disturbance, then eq 1 describes a linear model. Otherwise, three parameters in this model need to be determined with a nonlinear least-squares method. The nonlinear curve of the model surface based on the relationship of T_{ao} , F_{cw} , and F_a is shown in Figure 4. It is obvious that a conventional PID control algorithm is best suited for linear systems. The performance of a cooling-coil controller can vary when operating conditions change. A well-tuned PID controller for one set of environmental conditions may become sluggish or oscillatory at a different set of conditions.¹⁵

Therefore, a two-level control structure is proposed. In the lower level, a conventional PID controller is adopted:

$$\Delta u(k) = K_p [e(k) - e(k-1)] + K_i e(k) + K_d [e(k) - 2e(k-1) + e(k-2)]$$

Rewrite the incremental PID controller as

$$\Delta u(k) = w_0 e(k) + w_1 e(k-1) + w_2 e(k-2) \quad (3)$$

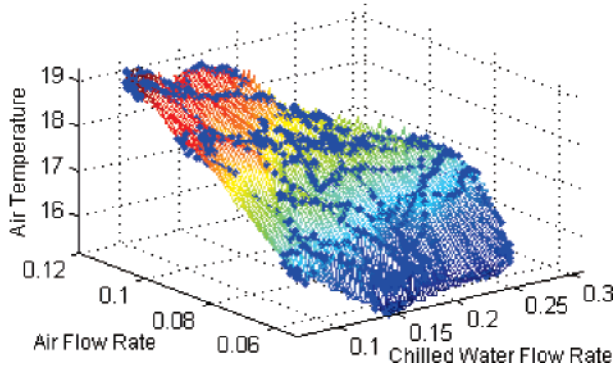


Figure 4. Nonlinear curve of the AHU model surface.

where $w_0 = K_p + K_i + K_d$, $w_1 = -K_p - 2K_d$, and $w_3 = K_d$.

To cope with the nonlinear dynamic behavior of a cooling-coil system and adapt a wide range of operating conditions, it is necessary to explore a time-varying lower level controller.

For this purpose, we rewrite the lower level controller as

$$\Delta u(k) = w_0(k) e(k) + w_1(k) e(k-1) + w_2(k) e(k-2)$$

Suppose that this time series is the output of a linear time-varying adaptive finite impulse response filter

$$\Delta u(k) = \sum_{i=0}^2 w_i(k) e(k-i) = \mathbf{W}^T(k) \mathbf{e}(k) \quad (4)$$

where $\mathbf{W}^T(k) = [w_0(k), w_1(k), w_2(k)]$ and $\mathbf{e}(k) = [e(k), e(k-1), e(k-2)]^T$.

If operating conditions vary in a narrow range, the lower level controller parameters are fixed, i.e., $w_i(k) = w_i(k-1)$, or the higher level algorithm optimizes the lower level controller parameters.

3. Receding-Horizon Optimal PID Controller

A cooling-coil system can be represented by the following CARIMA (controlled autoregressive and integrated moving average) model:

$$A(z^{-1}) y(k) = B(z^{-1}) u(k-1) + C(z^{-1}) \xi(k)/\Delta$$

where A , B , and C are polynomials in the backward shift operator z^{-1} of degrees n_a , n_b , and n_c , respectively. $\xi(k)$ is an external white noise disturbance with zero mean and variance σ^2 .

The j -step output of the system for the process can be derived by using two *Diophantine* equations

$$y(k+j) = \frac{E_j B}{C} \Delta u(k+j-1) + \frac{H_j}{C} y(k) + \frac{F_j}{C} y(k) + E_j \xi(k+j)$$

where E_j and F_j are polynomials in the backward shift operator z^{-1} of degrees $\min(j-1, n_c)$ and $n_c - j$, respectively.¹⁶ With this expectation, the j -step predictor for the process output becomes

$$\hat{y}(k+j|k) = G_j \Delta u(k+j-1) + H_j \Delta \bar{u}(k-1) + F_j \bar{y}(k)$$

where G_j and H_j are polynomials in the operator z^{-1} of degrees $j-1$ and $\max(n_{EB} - j + 1, n_c - 1)$ and $\Delta \bar{u}(k-1)$

$= [\Delta u(k-1)]/C$ and $\bar{y}(k) = y(k)/C$, where C is assumed to be a minimum phase.

Supposing that $C(z^{-1}) = 1$, the j -step predictor is as follows:

$$\hat{y}(k+j|k) = G_j \Delta u(k+j-1) + H_j \Delta u(k-1) + F_j y(k)$$

When the future control action eq 4 is introduced into the j -step process output prediction, we obtain

$$\hat{y}(k+j|k) = G_j \left[\sum_{i=0}^2 w_i(k+j-1) e(k+j-i-1) \right] + H_j \Delta u(k-1) + F_j y(k)$$

Therefore, the lower level PID control parameters can be obtained through minimization of a GPC criterion on a moving-horizon scenario.

To find optimal parameters $\{w_0^*(k), w_1^*(k), w_2^*(k)\}$, a multistage cost function is defined at every sample time k

$$J = E \left\{ \sum_{j=N_0}^{N_1} [\hat{y}(k+j|k) - r(k+j)]^2 + \sum_{j=1}^{N_u} \lambda(j) [\Delta u(k+j-1)]^2 \right\} \quad (5)$$

where $\hat{y}(k+j|k)$ is the predicted output j steps into the future at time k , $r(k+j)$ is the future reference trajectory, N_0 and N_1 are the minimum and maximum predictive horizons, respectively, N_u is the control horizon, and $N = N_1 - N_0 = N_u$.

Note that $J(k, W)$ is an index performance at time k . Substituting eq 4 into eq 5 results in

$$J(k, W) = E \left\{ \sum_{j=1}^N [\epsilon(k, W)]^2 + \sum_{j=1}^N \lambda(j) [\mathbf{W}^T(k+j-1) \mathbf{e}(k+j-1)]^2 \right\}$$

Assume that the set point is constant, i.e., $r(k) = r(k+j)$, where

$$\epsilon(k, W) = r(k) - \hat{y}(k+j|k)$$

and $\mathbf{W}^*(k-1)$ is the optimal parameter vector based on the minimization of the $J(k-1, W)$ criterion. When the index performance of eq 5 is computed up to an $k-1$ instant, it will fulfill the condition

$$\left. \frac{\partial J(k-1, W)}{\partial W} \right|_{W^*(k-1)} = 0 \quad (6)$$

For the sake of finding an optimal solution at time instant k , a second-order *Taylor* expansion of $J(k, W)$ over $\mathbf{W}^*(k-1)$ is given by

$$J(k, W) \approx J(k, W^*(k-1)) + \left. \frac{\partial J(k, W)}{\partial W} \right|_{W^*(k-1)} [\mathbf{W} - \mathbf{W}^*(k-1)] + \frac{1}{2} [\mathbf{W} - \mathbf{W}^*(k-1)]^T \left. \frac{\partial^2 J(k, W)}{\partial W^2} \right|_{W^*(k-1)} [\mathbf{W} - \mathbf{W}^*(k-1)] + O(|\mathbf{W} - \mathbf{W}^*(k-1)|^3) \quad (7)$$

$O(W)$ is the high-order expansion term, which will be small and can be omitted if $\mathbf{W}^*(k-1)$ is the optimal solution for the time instant $k-1$. Minimization of eq 7 with respect to W gives

$$\mathbf{W}^*(k) = \mathbf{W}^*(k-1) - \left[\frac{\partial^2 J(k, W)}{\partial W^2} \right]_{W^*(k-1)}^{-1} \left[\frac{\partial J(k, W)}{\partial W} \right]_{W^*(k-1)} \quad (8)$$

and the AT controller algorithm is obtained as (see the appendix for detailed derivations)

$$\mathbf{W}^*(k) = \mathbf{W}^*(k-1) + \mathbf{P}(k) \{ \epsilon[k, \mathbf{W}^*(k-1)] \mathbf{S}[k, \mathbf{W}^*(k-1)] - \lambda [\mathbf{W}^*(k-1)]^T \mathbf{e}(k) \mathbf{e}(k) \} \quad (9a)$$

$$\mathbf{P}(k) = \mathbf{Q}(k) - \lambda \frac{\mathbf{Q}(k) \mathbf{e}(k) \mathbf{e}^T(k) \mathbf{Q}(k)}{\lambda \mathbf{e}^T(k) \mathbf{Q}(k) \mathbf{e}(k) + 1} \quad (9b)$$

$$\mathbf{Q}(k) = \mathbf{P}(k-1) - \lambda \frac{\mathbf{P}(k-1) \mathbf{S}(k) \mathbf{S}^T(k) \mathbf{P}(k-1)}{\lambda \mathbf{S}^T(k) \mathbf{P}(k-1) \mathbf{S}(k) + 1} \quad (9c)$$

$$\hat{y}(k+j|k) = G_j \{ [\mathbf{W}^*(k-1)]^T \mathbf{e}(k) \} + H_j \Delta u(k-1) + F_j y(k) \quad (9d)$$

At time k , the lower level controller $\Delta u(k)$ is given by $W(k)$; then execute the system. Next time, a new control action $\Delta u(k+1)$ is recalculated by the estimated model and system criterion on a moving-horizon window. Because the estimated model and system criterion is the same as that for a standard GPC algorithm, better control quality can be obtained by the proposed strategy than by a conventional PID controller. The purpose of taking a new measurement at each time step is to obtain the optimal parameters and compensate for unmeasured disturbances and model inaccuracy, both of which cause the measured system output to be different from that predicted by the model. The optimal control action that minimizes the cost function will be derived from now on and updated throughout a wide range of operating conditions.

Hence, some conclusions are as follows:

Remark 1 (Practicability). Our choice of presenting this particular design is motivated by its explicit structure and well-defined stability. Any processes with a conventional PID control algorithm can utilize the proposed strategy to cope with a wide range of operating conditions. Because the system hardware and the definitions of the controller parameters do not need to be changed, the method can be easily grasped by process engineers.

Remark 2 (Robustness). As long as the weight $\lambda(\cdot)$ is positive definite, the proposed algorithm can provide a robust design. Here, an estimated model is adopted in the control receding calculation, and the plant-model mismatch is considered in a GPC objective function. The philosophy is to decrease the weight influence on the control action in the objective function in the case of large model mismatch.

Remark 3 (Stability). Because of stability considerations, we should choose an infinite prediction horizon. Usually, three “ingredients”, which include a terminal cost, a terminal constraint set, and a local controller, have been found to be useful in developing stabilize model predictive controllers.¹⁷



Figure 5. Plant of a centralized HVAC system.

Remark 4 (Computation Complexity). Because the existing computational resource is similar to that of the conventional MPC, the proposed algorithm does not bear the burden of computation. The difference between them is the objective function. Besides, only the system performance deteriorates in a wide range of operating conditions, and the controller parameters tuning procedure starts to work.

The AT predictive PID controller algorithm is given as follows:

Step 1: Estimate the CARIMA model to yield G , H , E , and F , and set the maximum and minimum predictive horizons and control horizon.

Step 2: Take $k = 0$, $W^*(0) = 0$, and $P(0) = I$.

Step 3: Calculate the predictive output $\hat{y}(k+j|k)$.

Step 4: Compute $W^*(k)$ based on eq 9.

Step 5: Determine the control action by $\Delta u(k) = [\mathbf{W}^*(k)]^T \mathbf{e}(k)$.

Step 6: Set $k = k + 1$, and go back to step 1.

Thereby, the optimal parameters are retuned to update the conventional PID controller parameters.

4. Simulation and Experimental Results

The experiment is conducted on a centralized HVAC system (shown in Figure 5) that has three chillers, three zones with three AHUs, three cooling towers, and flexible partitions of up to 12 rooms. All motors (fans, pumps, and compressors) are controlled by variable-speed drives.

The cooling-coil system consists of two rows and dimensions of 25 cm × 25 cm × 8 cm (shown in Figure 6). The measurement signals for the experiment are the water and air flow rates, on-coil air dry-bulb/web-bulb temperatures, and cooling-coil inlet and outlet water temperatures. The experiment is implemented under the following conditions: fixed chilled water supply temperature and cooling load variation caused by the air and water flow rates (illustrated in Table 1).

In the simulation and experiment, the Chien–Hrones–Reswick tuning rule¹⁸ is adopted to obtain PI controller parameters because of its universality and high availability in industrial processes.

Different models have been tested to verify the control algorithm effectiveness in a variety of realistic operating conditions. Suppose that the model switches at the times $t = 3000$ and 6000 s. As can be seen in Figure 7, a larger overshoot and long setting time are obtained by a conventional PID control algorithm than by the receding-horizon optimization strategy. A set of optimal PID

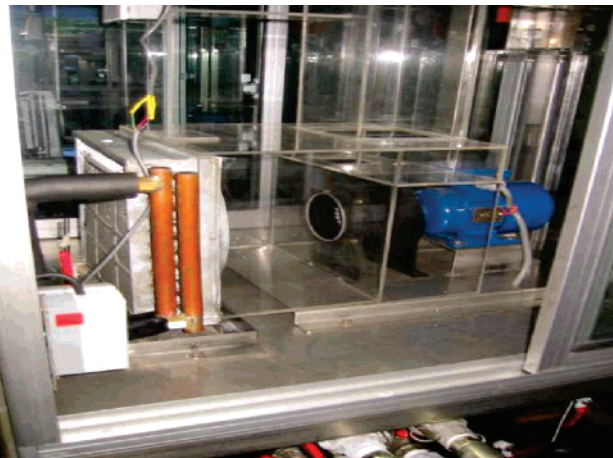


Figure 6. Cooling-coil system.

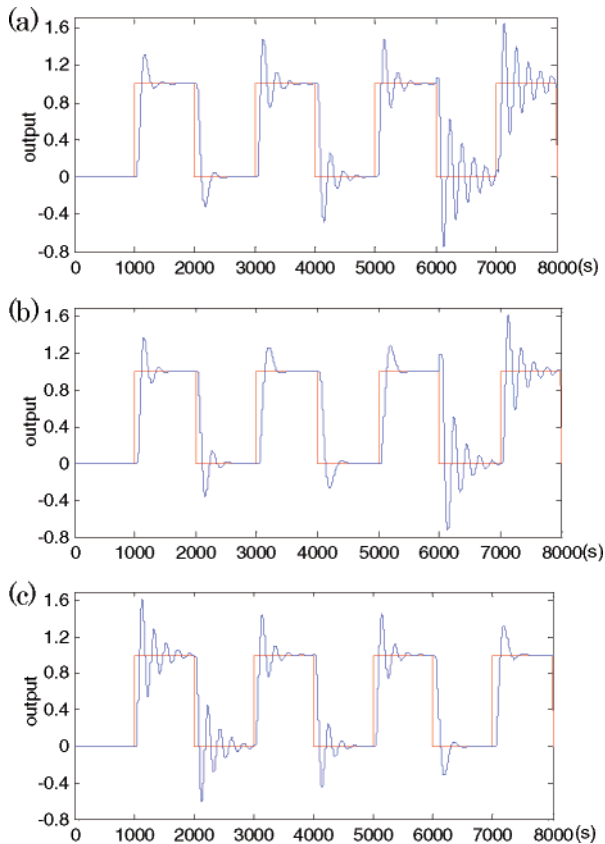


Figure 7. (a) Designed by the model of the first region. (b) Designed by the model of the second region. (c) Designed by the model of the second region.

parameters is designed on the basis of the first region operating conditions. It is seen from Figure 7a that the nonlinear system response in the first region has a few overshoots and faster setting time in comparison with that of other regions. The same, only 18% overshoots and 200 s rise time, is obtained in the second region, and the results are shown in Figure 7b. The optimal controller parameters are designed on the basis of the second region operating conditions. No large oscillation

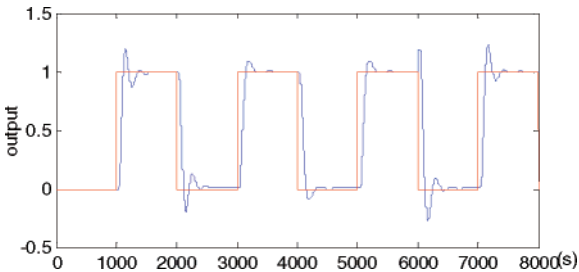


Figure 8. Designed with a non-AT predictive PID.

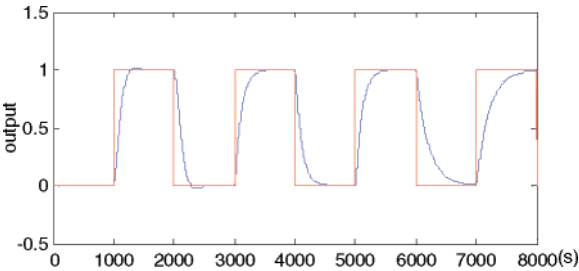


Figure 9. Designed with receding-horizon optimization.

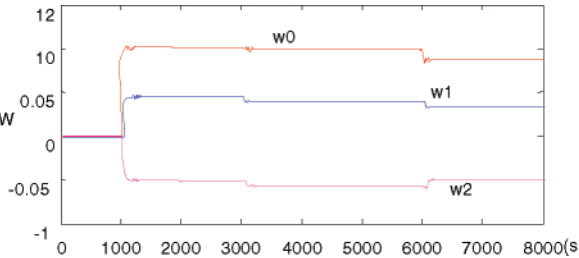


Figure 10. PID parameters w_0 , w_1 , and w_2 .

is achieved for the third region compared with other regions (shown in Figure 7c), and the results are shown in Figure 7c. As can be seen in Figure 7, a conventional PID controller designed by a nominal model may not obtain satisfactory control quality for a plant with a wide range of operating conditions.

On the basis of the model in the second region, the results (shown in Figure 8) using a predictive PID method appear to be a large oscillation and overshoots. Compared with a well-tuned conventional PID controller, the rise time is smaller for its model prediction. However, the robustness of the system is weak in the presence of a disturbance. Figure 9 exhibits a satisfactory tradeoff between achieving a fast and nonoscillatory convergence of the controlled output toward the set point and supplying smooth feasible control actions. The variations of lower level controller parameters are shown in Figure 10.

Figures 11–13 show the different responses of a conventional PID controller and AT predictive PID controller for the case of temperature set-point change and air flow rate fluctuation.

First, we let the off-coil temperature stabilize at 18.7 °C, when the air flow rate is 60% of the full range, and then the set points go up to 19.5 °C at time $t = 250$ s.

Second, when the air flow rate is decreased to 40% of the full range, which leads to an increase in the flow

Table 1. Model Parameters

region	load range (kW)	c_1	c_2	e	a_1	b_0	b_1	b_2	K_p	K_i
first	[0.40, 0.75]	0.7132	0.5402	0.8	[−0.3292, −0.4092]	[55.48, 50.1]	[38.43, 37.07]	[0, 0]	11.38	0.0078
second	[0.75, 1.00]	0.7076	0.6499	0.8	[−0.3679, −0.4346]	[13.96, 13.03]	[61.69, 60.35]	[7.167, 7.475]	8.384	0.0074
third	[1.00, 1.20]	0.7403	0.9183	0.8	[−0.3858, −0.4493]	[49.01, 46.75]	[35.75, 36.85]	[0, 0]	7.565	0.0057

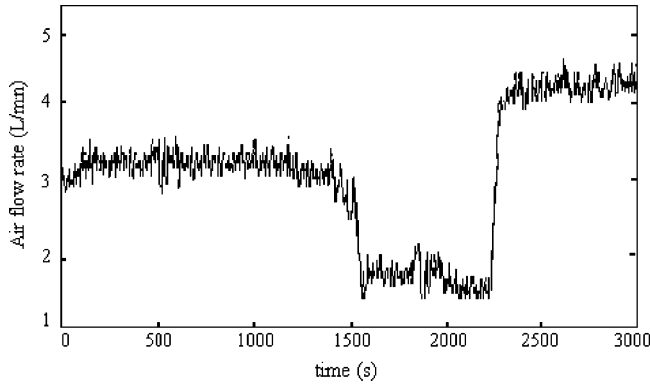


Figure 11. Change of the air flow rate for the experiment.

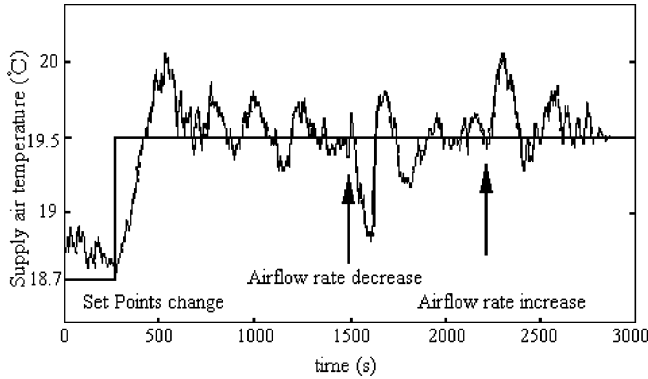


Figure 12. Temperature using a conventional PID control method.

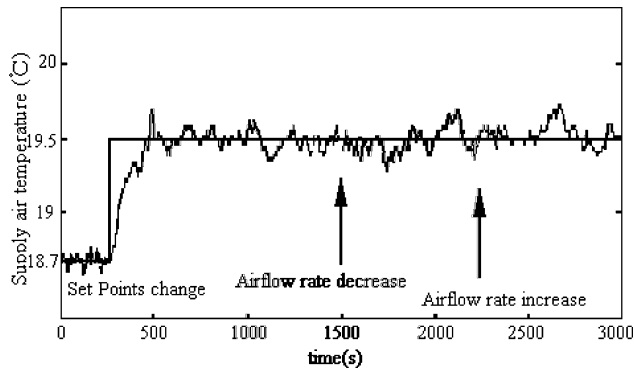


Figure 13. Temperature using a receding-horizon optimization algorithm.

rate of the cooling water, the set point of the temperature is the same at time $t = 1500$ s.

Third, when the air flow rate is increased to 80% of the full range, which leads to a decrease in the flow rate of the cooling water, the set point of the temperature is the same at time $t = 2200$ s.

Figures 11 and 12 give comparisons of the proposed controller and a well-tuned PID controller in the cooling-coil system. It is shown that the proposed strategy has a faster rise time and smaller temperature variations. As can be seen in the figures, the overshoot is only up to 0.2 °C with the proposed algorithm, while that of a conventional PID control algorithm is larger than 0.7 °C.

We summarize the performances of the rise time and overshoots between the two methods (shown in Table 2). The simulation and results show that the proposed algorithm economizes the energy under the same conditions.

Table 2. Performance Comparison

testing	criteria	conventional PID parameter	predictive PID parameter
set-point change	overshoot (°C)	0.6	0.15
	settling time (s)	650	250
disturbance (flow rate increase)	max error (°C)	-0.6	-0.2
	settling time (s)	430	270
disturbance (flow rate decrease)	max error (°C)	0.6	0.2
	settling time (s)	460	250

5. Conclusions

Because of human error or time drifting, a well-tuned PID controller will heavily deteriorate the system performance. Although many methods are developed to detune the PID controller, it is very difficult to obtain optimal settings because it is not easy for the process engineer to understand the advanced strategy. Hence, a novel receding-horizon optimization strategy with two level control structures, based on the GPC criterion and CARIMA model, has been designed for a cooling-coil system. The purpose of the higher level is to minimize the sum of square errors between the predicted and desired output trajectories with an additional term weighting the projected control increment. Through minimization of the criterion and tuning of the lower level PID controller parameters, a satisfied control quality can be obtained for a wide range of operating conditions. Simulation and experiments show that the proposed controller can rapidly reject the effects of both static and dynamic disturbances. The performance of a cooling-coil system is improved compared with that of a conventional PID controller. We have also shown that energy economics in the HVAC system can be effectively implemented by the proposed control scheme.

Acknowledgment

This work was supported by the National Natural Science Foundation of China under Grant 60474051 and the Key Technology and Development Program of Shanghai Science and Technology Department under Grant 04DZ11008 and partly by the Specialized Research Fund for the Doctoral Program of Higher Education of China (Grant 20020248028). The authors are grateful to anonymous reviewers for their valuable recommendations.

Appendix

The criterion given by eq 5 can be rewritten as

$$\begin{aligned}
 J(k, W) &= [\mathbf{r} - \hat{\mathbf{y}}]^2 + \lambda [\mathbf{u}]^2 \\
 &= \epsilon(k, W)^T \epsilon(k, W) + \lambda [W^T(k) \mathbf{e}(k)]^T [W^T(k) \mathbf{e}(k)]
 \end{aligned} \quad (10)$$

where

$$\mathbf{r}^T = [r(t+1), \dots, r(t+N)]$$

$$\mathbf{y}^T = [\hat{y}(t+1), \dots, \hat{y}(t+N)]$$

$$\mathbf{u}^T = [\Delta u(k), \dots, \Delta u(k+N-1)]$$

$$\epsilon(k, W) = r(k) - \hat{y}(k+j|k)$$

Differentiating this expression twice with respect to W , we obtain

$$\frac{\partial J(k, W)}{\partial W} = \epsilon(k, W) \frac{\partial \epsilon(k, W)}{\partial W} + \lambda W^T(k) e(k) \frac{\partial [W^T(k) e(k)]}{\partial W} + \frac{\partial J(k-1, W)}{\partial W} \quad (11a)$$

$$\frac{\partial^2 J(k, W)}{\partial W^2} = \epsilon(k, W) \frac{\partial^2 \epsilon(k, W)}{\partial W^2} + \frac{\partial \epsilon(k, W)}{\partial W} \frac{\partial \epsilon(k, W)}{\partial W} + 2\lambda e(k) e^T(k) + \frac{\partial^2 J(k-1, W)}{\partial W^2} \quad (11b)$$

where

$$\epsilon(k, W) = r(k+j) - \hat{y}(k+j|k)$$

$$\frac{\partial [W^T(k) e(k)]}{\partial W} = \frac{\partial W^T}{\partial W} e(k) + \frac{\partial e^T}{\partial W} W(k) = e(k)$$

Because $W^*(k-1)$ is optimal at $k-1$, the following equation holds:

$$\left. \frac{\partial J(k-1, W)}{\partial W} \right|_{W^*(k-1)} = 0 \quad (12)$$

When eq 12 is substituted into eq 11a, the first derivative at $W^*(k-1)$ can be written as

$$\left. \frac{\partial J(k, W)}{\partial W} \right|_{W^*(k-1)} = \epsilon[k, W^*(k-1)] \left. \frac{\partial \epsilon(k, W)}{\partial W} \right|_{W^*(k-1)} + \lambda [W^*(k-1)]^T e(k) e(k) \quad (13)$$

The optimal $W^*(k)$ is very close to $W^*(k-1)$, because k is big enough, and then the following approximation is correct:

$$\left\{ \begin{aligned} O[W^*(k) - W^*(k-1)] &\rightarrow 0 \\ \left. \frac{\partial^2 J(k, W)}{\partial W^2} \right|_{W^*(k-1)} &\approx \left. \frac{\partial^2 J(k, W)}{\partial W^2} \right|_{W^*(k)} \end{aligned} \right. \quad (14)$$

Using eqs 8, 13, and 14, the optimal vector $W^*(k)$ is written as

$$W^*(k) = W^*(k-1) + R(k)^{-1} \{ \epsilon[k, W^*(k-1)] S[k, W^*(k-1)] - \lambda [W^*(k-1)]^T e(k) e(k) \} \quad (15)$$

where

$$\left\{ \begin{aligned} R(k) &= \left. \frac{\partial^2 J(k, W)}{\partial W^2} \right|_{W^*(k)} \\ S[k, W^*(k-1)] &= - \left. \frac{\partial \epsilon(k, W)}{\partial W} \right|_{W^*(k-1)} \end{aligned} \right. \quad (16)$$

To avoid the matrix inversion in eq 15, a known lemma will be used in the procedure of computing the optimal control variable.¹⁹ Therefore, substituting eq 14 into eq 16 and applying the lemma results in

$$R(k) = R(k-1) + S[k, W^*(k-1)] S[k, W^*(k-1)]^T + 2\lambda e(k) e(k)^T$$

Therefore

$$\begin{aligned} R(k)^{-1} &= \{ R(k-1) + S[k, W^*(k-1)] S[k, W^*(k-1)]^T \}^{-1} - \\ &\quad \{ R(k-1) + S[k, W^*(k-1)] S[k, W^*(k-1)]^T \}^{-1} e(k) \\ &\quad \{ e(k)^T \{ R(k-1) + S[k, W^*(k-1)] S[k, W^*(k-1)]^T \}^{-1} + \\ &\quad 1/\lambda \}^{-1} e(k) \{ R(k-1) + \\ &\quad S[k, W^*(k-1)] S[k, W^*(k-1)]^T \}^{-1} \end{aligned}$$

Denoting

$$P(k) = R(k)^{-1} \quad \text{and}$$

$$Q(k) = \{ R(k-1) + S[k, W^*(k-1)] S[k, W^*(k-1)]^T \}^{-1}$$

then

$$P(k) = Q(k) - \lambda \frac{Q(k) e(k) e^T(k) Q(k)}{\lambda e^T(k) Q(k) e(k) + 1}$$

which is eq 9b.

Apply the known lemma about matrix inversion again, giving assignment

$$\begin{aligned} Q(k) &= \{ R(k-1)^{-1} - R(k-1)^{-1} S[k, W^*(k-1)] \\ &\quad \{ S[k, W^*(k-1)]^T R(k-1)^{-1} S[k, W^*(k-1)] + \\ &\quad 1/\lambda \}^{-1} [S[k, W^*(k-1)]^T R(k-1)^{-1}] \}^{-1} \end{aligned}$$

Thus

$$Q(k) = P(k-1) - \lambda \frac{P(k-1) S(k) S^T(k) P(k-1)}{\lambda S^T(k) P(k-1) S(k) + 1}$$

which is eq 9c.

Literature Cited

- (1) ASHRAE. *ASHRAE handbook—fundamentals*; American Society of Heating, Refrigerating and Air-Conditioning Engineers Inc.: Atlanta, GA, 1997.
- (2) Astrom, K. J.; Hagglund, T. *PID Controllers: theory, design, and tuning*; Instrument Society of America: Research Triangle Park, NC, 1995.
- (3) Prabhat, A.; Lakshminarayanan, S. Tuning proportional–integral–derivative controllers using achievable performance indices. *Ind. Eng. Chem. Res.* **2003**, 42 (22), 5576–5582.
- (4) Rahmati, A.; Rashidi, F.; Rashidi, M. A hybrid fuzzy logic and PID controller for control of nonlinear HVAC systems, *IEEE International Conference on Systems, Man and Cybernetics*; IEEE: Piscataway, NJ, 2003; pp 2249–2254.
- (5) Wu, J.; Cai, W. J. Development of an adaptive neuro-fuzzy method for supply air pressure control in HVAC system. *IEEE International Conference on Systems, Man and Cybernetics*; IEEE: Piscataway, NJ, 2000; pp 3806–3809.
- (6) Nassif, N.; Kaji, S.; Sabourin, R. Evolutionary algorithm for multi-objective optimization in HVAC system control strategy. *IEEE Annual Meeting of Fuzzy Information*; IEEE: Piscataway, NJ, 2004; pp 51–56.
- (7) Chow, T. T.; Zhang, Q. G.; Lin, Z.; Song, C. L. Global optimization of absorption chiller system by genetic algorithm and neural network. *Energy Buildings* **2002**, 34 (1), 103–109.
- (8) Bi, Q.; Cai, W. J.; et al. Advanced controller auto-tuning and its application in HVAC systems. *Control Eng. Pract.* **2000**, 8 (2), 633–644.
- (9) Dexter, A. L.; Hayes, P. A robust self-tuning controller for HVAC applications. *ASHRAE Trans.* **1989**, 2, 431–439.
- (10) Qin, S. J.; Badgwell, T. A. A survey of industrial model predictive control technology. *Control Eng. Pract.* **2003**, 11 (7), 733–764.

- (11) Virk, G. S.; Loveday, D. L. A comparison of predictive, PID and on/off control techniques for energy management control. *ASHRAE Trans.* **1991**, *97* (2), 3–10.
- (12) Jorgl, H. P.; Pargfrieder, J. An integrated control system for optimizing the energy consumption and user comfort in buildings. *IEEE International Symposium on Computer Aided Control System Design Proceedings*, Glasgow, Scotland, U.K., Sept 2002; IEEE: Piscataway, NJ, 2002; pp 127–132.
- (13) Cho, S. H.; Zaheer, M. Predictive control of intermittently operated radiant floor heating systems. *Energy Convers. Manage.* **2003**, *44* (8), 1333–1342.
- (14) Lu, L.; Cai, W. J.; et al. HVAC system optimization—condenser water loop. *Energy Convers. Manage.* **2004**, *45* (4), 613–663.
- (15) Salsbury, T. I. A temperature controller for VAV air-handling units based on simplified physical models. *ASHRAE HVAC&R Res. J.* **1998**, *4* (3), 200–214.
- (16) Clarke, D. W. Generalized Predictive Control. *Automatica* **1987**, *23* (5), 149–16.
- (17) Mayne, D. Q.; Rawlings, J. B.; et al. Constrained model predictive control: stability and optimality. *Automatica* **2000**, *36* (6), 789–814.
- (18) Cohen, G. H.; Coon, G. A. Theoretical consideration of retarded control. *ASHRAE Trans.* **1953**, *75* (2), 827–834.
- (19) Ljung, L.; Soderstrom, T. *Theory and practices of recursive identification*; MIT Press: Cambridge, MA, 1983; pp 24–33.

Received for review January 18, 2004

Revised manuscript received January 20, 2005

Accepted February 7, 2005

IE0499411